Electronic Supplementary Information (ESI)

Single ion magnets based on lanthanoid polyoxomolybdate complexes

José J. Baldoví,[a†] Yan Duan,[a†] Carlos Juan Bustos,[b,c] Salvador Cardona-Serra,[d] Pierre Gouzerh,[c] Richard Villanneau,[c] Geoffrey Gontard,[c] Juan M. Clemente-Juan,[a] Alejandro Gaita-Ariño,[a*] Carlos Giménez-Saiz,[a*] Anna Proust[c*] and Eugenio Coronado[a*]

[a.] Instituto de Ciencia Molecular (ICMol), Universidad de Valencia, C/Catedrático José Beltran, 2, E-46980 Paterna, Spain.

[b.] Facultad de Ciencia, Instituto de Química, Campus Isla Teja, Universidad Austral de Chile, Valdivia, Chile.

[c.] Sorbonne Universites, UPMC-Paris 06, UMR 8232, Institut Parisien de Chimie Moléculaire, 4 Place Jussieu, F-75005 Paris, France.

[d.] Trinity College Dublin, College Green, Dublin 2, Ireland.

1. Elemental analysis results

$LnMo_{16}$ series

TBA = $(n\text{-}C_4H_9)_4N$

$[TBA]_5[Tb(Mo_8O_{26})_2]$ ($TbMo_{16}$): (0.487 g, 65.7%). Elemental analysis calcd (%) for $C_{80}H_{180}N_5TbMo_{16}O_{52}$: C, 25.70; H, 4.85; N, 1.87. Found: C, 25.05; H, 5.11; N, 1.82. The Tb/Mo ratio obtained by SEM-EDX (scanning electron microscope with energy-dispersive X-ray analysis) are in agreement with the above formula obtained from the structure refinement (found: Tb/Mo = 8.85:91.15, calcd: Tb/Mo = 9.21:90.79).

$[TBA]_5[Dy(Mo_8O_{26})_2]$ ($DyMo_{16}$): (0.453 g, 59.8%). Elemental analysis calcd (%) for $C_{80}H_{180}N_5DyMo_{16}O_{52}$: C, 25.68; H, 4.85; N, 1.87. Found: C, 25.14; H, 4.91; N, 2.00; The Dy/Mo ratio: found: Dy/Mo = 9.40:90.60, calcd: Dy/Mo = 9.47:90.53.

$[TBA]_5[Ho(Mo_8O_{26})_2]$ ($HoMo_{16}$): (0.513 g, 67.7%). Elemental analysis calcd (%) for $C_{80}H_{180}N_5HoMo_{16}O_{52}$: C, 25.66; H, 4.86; N, 1.87; Found: C, 24.95; H, 4.87; N, 1.90; The Ho/Mo ratio: found: Ho/Mo = 10.58: 89.42, calcd: Ho/Mo = 9.53: 90.47.

$[TBA]_5[Er(Mo_8O_{26})_2]$ ($ErMo_{16}$): (0.492 g, 64.9%). Elemental analysis calcd (%) for $C_{80}H_{180}N_5ErMo_{16}O_{52}$: C, 25.65; H, 4.84; N, 1.87. Found: C, 25.30; H, 4.98; N, 1.88; The Er/Mo ratio: found: Er/Mo = 9.90:90.10, calcd: Er/Mo = 9.58:90.42.

$[TBA]_5[Tm(Mo_8O_{26})_2]$ ($TmMo_{16}$): (0.437 g, 57.6%). Elemental analysis calcd (%) for $C_{80}H_{180}N_5TmMo_{16}O_{52}$: C, 25.64; H, 4.84; N, 1.87. Found: C, 25.96; H, 5.04; N, 1.85; The Tm/Mo ratio: found: Tm/Mo = 10.94:89.06, calcd: Tm/Mo = 9.73:90.27.

$[TBA]_5[Yb(Mo_8O_{26})_2]$ ($YbMo_{16}$): (0.465 g, 61.2%). Elemental analysis calcd (%) for $C_{80}H_{180}N_5YbMo_{16}O_{52}$: C, 25.61; H, 4.84; N, 1.87. Found: C, 24.72; H, 4.89; N, 1.85; The Yb/Mo ratio: found: Yb/Mo = 9.63:90.37, calcd: Yb/Mo = 9.99:90.01.

$LnMo_{10}$ series

$[TBA]_3[Tb\{Mo_5O_{13}(MeO)_4(NNC_6H_4\text{-}p\text{-}NO_2)\}_2]\cdot 1.5CHCl_3$ ($TbMo_{10}$): (0.283 g, 80.6 %). Elemental analysis calcd (%) for $C_{69.5}H_{141.5}N_9O_{38}Cl_{4.5}Mo_{10}Tb$: C, 27.92; H, 4.77; N, 4.22; found: C, 27.97; H, 4.85; N, 4.12.

$[TBA]_3[Dy\{Mo_5O_{13}(MeO)_4(NNC_6H_4\text{-}p\text{-}NO_2)\}_2]\cdot 1.5CHCl_3$ ($DyMo_{10}$): (0.309 g, 87.9%). Elemental analysis calcd (%) for $C_{69.5}H_{141.5}N_9O_{38}Cl_{4.5}Mo_{10}Dy$: C, 27.89; H, 4.77; N, 4.21; found: C, 27.73; H, 4.71; N, 4.05.

$[TBA]_3[Ho\{Mo_5O_{13}(MeO)_4(NNC_6H_4\text{-}p\text{-}NO_2)\}_2]\cdot 1.5CHCl_3$ ($HoMo_{10}$): (0.325 g, 92.3%). Elemental analysis calcd (%) for $C_{69.5}H_{141.5}N_9O_{38}Cl_{4.5}Mo_{10}Ho$: C, 27.92; H, 4.77; N, 4.22; found: C, 27.97; H, 4.85; N, 4.12.

$[TBA]_3[Er\{Mo_5O_{13}(MeO)_4(NNC_6H_4\text{-}p\text{-}NO_2)\}_2]\cdot 1.5CHCl_3$ ($ErMo_{10}$): (0.243 g, 69.0 %). Elemental analysis calcd (%) for $C_{69.5}H_{141.5}N_9O_{38}Cl_{4.5}Mo_{10}Er$: C, 27.85; H, 4.76; N, 4.21; found: C, 27.68; H, 4.76; N, 4.07.

$[TBA]_3[Yb\{Mo_5O_{13}(MeO)_4(NNC_6H_4\text{-}p\text{-}NO_2)\}_2]\cdot 1.5CHCl_3$ ($YbMo_{10}$): (0.321 g, 91.0 %). Elemental analysis calcd (%) for $C_{69.5}H_{141.5}N_9O_{38}Cl_{4.5}Mo_{10}Yb$: C, 27.79; H, 4.75; N, 4.20; found: C, 28.03; H, 4.80; N, 4.32.

$[TBA]_3[Nd\{Mo_5O_{13}(MeO)_4(NNC_6H_4\text{-}p\text{-}NO_2)\}_2]\cdot 1.5CHCl_3$ ($NdMo_{10}$): (0.330 g, 94.6%). Elemental analysis calcd (%) for $C_{69.5}H_{141.5}N_9O_{38}Cl_{4.5}Mo_{10}Nd$: C, 28.06; H, 4.79; N, 4.24; found: C, 28.46; H, 4.93; N, 4.32.

2. IR spectra

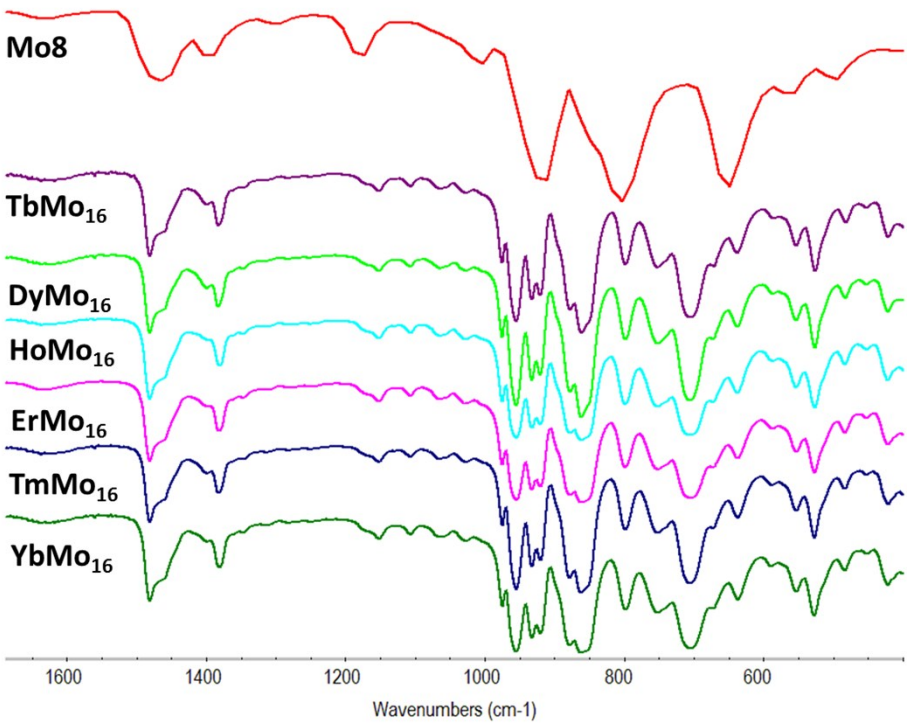

Fig. S1. FT-IR spectra of the precursor $[TBA]_4[\beta\text{-}Mo_8O_{26}]$ and the $LnMo_{16}$ series, where Ln^{III} = Tb, Dy, Ho, Er, Tm and Yb, in the range of 1700-400 cm^{-1}.

3. Crystal structure determination

$LnMo_{16}$ series

Crystals of $LnMo_{16}$ are extremely efflorescent and solvent loss occurs immediately after they are separated from their mother solutions. Therefore, although the crystals were quickly covered with Paratone-N oil and placed in a stream of cooled nitrogen (120 K), some partial loss of solvent from the crystal could not be avoided. This fact causes a lowering in the quality of the single crystals as well as a large disorder in some of the organic cations present in the crystals (see below). A Nonius-Kappa CCD single-crystal diffractometer equipped with graphite-monochromated Mo Kα radiation (λ = 0.71073 Å) was used for data collection. The CrysAlis software package[1] was used for data collection routines, unit cell refinements, and data processing. Structure solution and refinement were carried out using SHELXS-97 and SHELXL-97.[2] The asymmetric units of $LnMo_{16}$ contain one complete polyoxometalate anion and five tetrabutylammonium ($[(n\text{-}C_4H_9)_4N]^+$, TBA^+ in short) cations. The structure solution reveals that some TBA^+ cations are extremely disordered, exhibiting unusually high isotropic thermal parameters. This fact was attributed to thermal liberation caused by the loss of solvent molecules from the crystal, which creates voids in the surroundings of these TBA^+ cations. Attempts of modelling this disorder using the facilities included in SHELXL-97 (PART, DELU and SIMU instructions) did not result in lower thermal parameters and even gave rise to unstable refinements in some cases. Therefore, only a small fraction of the disorder found in the butyl chains of the cations was modeled using the PART instructions. In particular, all the crystal structures contain one of the five TBA^+ cations (labelled TBA5) was found to be so disordered that some of the isotropic thermal parameters of the carbon atoms could not be refined and had to be fixed to avoid their blowing up. In addition, in structure $ErMo_{16}$ some carbon atoms of this TBA^+ cation could be found in difference maps and then the whole cation was removed from the experimental structure factors and modeled using the SQUEEZE procedure.[3] Some acetonitrile molecules were also found in difference maps exhibiting large disorder and very high isotropic thermal factors. As they could not be modeled satisfactorily using atomic sites they were removed from the atomic list and their diffuse contribution was also

treated with the SQUEEZE program. This procedure gave void volumes and electron numbers per unit cell which correspond quite reasonably to 8 acetonitrile molecules per formula for all compounds in the series $LnMo_{16}$ except for the case of $TbMo_{16}$ where 6 acetonitrile molecules were found. All molybdenum and oxygen atoms were refined anisotropically in all six structures, while some TBA^+ cations were left isotropic. Hydrogen atoms on carbon atoms were included at calculated positions and refined with a riding model. Multi-scan or analytical numeric absorption corrections were applied to the data of $LnMo_{16}$ using the software integrated in the program CrysAlis. Crystallographic parameters for $LnMo_{16}$ are summarized in Table S1. Crystallographic data in cif format can be obtained with numbers CCDC 1446092-1446097 free of charge from the Cambridge Crystallographic Data Centre via www.ccdc.cam.ac.uk/data_request/cif.

$LnMo_{10}$ series

The molecular structures of the Tb, Dy, Ho, Er and Yb analogues of $LnMo_{10}$ were determined by X-ray diffraction after recrystallization in mixtures of $CHCl_3/Et_2O$ or $CHCl_3$/thf (thf = C_4H_8O).

Single crystals of each of the Tb, Dy, Ho, Er and Yb analogues of $LnMo_{10}$ were selected, mounted and transferred into a cold nitrogen gas stream. Intensity data was collected with a Bruker Kappa-APEX2 system using fine-focus sealed tube Mo-Kα radiation. Unit-cell parameters determination, data collection strategy, integration and absorption correction were carried out with the Bruker APEX2 suite of programs. The structures were solved using SIR92[4] (Tb, Ho, Er) or SHELXT-2014[2] (Dy, Yb) and refined anisotropically by full-matrix least-squares methods using SHELXL2013[2] (Tb, Ho, Er) or SHELXL2014[2] (Dy, Yb) within the WinGX suite[5]. The structures were deposited at the Cambridge Crystallographic Data Centre with numbers CCDC 1482838-1482842 and can be obtained free of charge via www.ccdc.cam.ac.uk.

The cell parameters of a crystal of $NdMo_{10}$ were measured and found to be isostructural to the Ho, Er and Yb derivatives.

Table S1. Crystallographic Data and Structure Refinement for compounds $LnMo_{16}$, where Ln^{III} = Tb, Dy, Ho, Er, Tm and Yb.

Compound		**$TbMo_{16}$**		**$DyMo_{16}$**		**$HoMo_{16}$**		**$ErMo_{16}$**		**$TmMo_{16}$**		**$YbMo_{16}$**	
Empirical formula		$C_{92}H_{198}Mo_{16}N_{11}O_{52}Tb$		$C_{96}H_{204}DyMo_{16}N_{13}O_{52}$		$C_{96}H_{204}HoMo_{16}N_{13}O_{52}$		$C_{96}H_{204}ErMo_{16}N_{13}O_{52}$		$C_{96}H_{204}Mo_{16}N_{13}O_{52}Tm$		$C_{96}H_{204}Mo_{16}N_{13}O_{52}Yb$	
Formula weight		3984.57		4070.26		4072.69		4075.02		4076.69		4080.80	
T/K		120(2)		120(2)		120(2)		120(2)		120(2)		120(2)	
Crystal system		Monoclinic		Orthorhombic		Orthorhombic		Orthorhombic		Orthorhombic		Orthorhombic	
Space group		$P\ 2_1/c$		P c a b		P c a b		P c a b		P c a b		P c a b	
a/Å	α/°	25.0421(7)	90	17.7626(4)	90	17.88390(15)	90	17.8110(3)	90	17.8375(2)	90	17.8722(3)	90
b/Å	β/°	17.1885(5)	91.419(2)	32.9141(8)	90	32.8402(2)	90	33.1580(5)	90	32.8499(4)	90	32.7932(5)	90
c/Å	γ/°	31.9702(9)	90	47.7196(12)	90	47.8961(4)	90	48.1554(8)	90	47.7986(8)	90	47.8651(7)	90
V/Å^3		13756.9(7)		27898.8(12)		28129.9(4)		28439.5(8)		28008.1(7)		28053.1(8)	
Z		4		8		8		8		8		8	
ρ_{calcd}/g cm^{-3}		1.924		1.938		1.923		1.903		1.934		1.932	
μ/mm^{-1}		1.991		1.995		2.010		2.022		2.087		2.118	
F(000)		7920		16200		16208		16216		16224		16232	
Crystal size / mm^3		0.2985 x 0.1639 x 0.0691		0.2702 x 0.0970 x 0.0719		0.469 x 0.250 x 0.121		0.20 x 0.15 x 0.08		0.2591 x 0.1485 x 0.0678		0.2296 x 0.1783 x 0.1755	
θ range for data collection		3.13° to 28.65°		3.07° to 28.23°		3.06° to 28.20°		1.05° to 27.47°		2.90° to 28.28°		3.06° to 28.23°	
		-33<=h<=32		-22<=h<=22		-23<=h<=22		-22<=h<=23		-23<=h<=22		-22<=h<=23	
Index ranges		-22<=k<=22		-43<=k<=40		-43<=k<=43		-41<=k<=42		-43<=k<=43		-43<=k<=43	
		-41<=l<=42		-63<=l<=56		-62<=l<=63		-60<=l<=61		-60<=l<=62		-60<=l<=62	
Reflections collected		126269		129978		296655		135509		164439		298597	
Independent reflections		32334 (R_{int}= 0.0863)		31723 (R_{int} = 0.1011)		33161 (R_{int} = 0.0417)		31298 (R_{int} = 0.1037)		32083 (R_{int} = 0.0711)		32999 (R_{int} = 0.0912)	
Completeness		0.982		0.970		0.993		0.961		0.996		0.998	
Max. and min. transmission		0.880 and 0.614		0.886 and 0.671		1.00000 and 0.75991		0.559 and 0.430		0.878 and 0.685		1.00000 and 0.78715	
Data / restraints / parameters		32334 / 50 / 1033		31723 / 93 / 963		33161 / 265 / 1330		31298 / 47 / 886		32083 / 79 / 1295		32999 / 47 / 1288	
Goodness-of-fit on F^2		1.084		1.043		1.228		1.023		1.091		1.093	
Final R indices [I > 2σ(I)]		R1 = 0.1205, wR2 = 0.3127		R1 = 0.1430, wR2 = 0.3186		R1 = 0.0904, wR2 = 0.1803		R1 = 0.0958, wR2 = 0.2688		R1 = 0.1116, wR2 = 0.2275		R1 = 0.1134, wR2 = 0.2363	
R indices (all data)		R1 = 0.1776, wR2 = 0.3448		R1 = 0.2018, wR2 = 0.3475		R1 = 0.1016, wR2 = 0.1844		R1 = 0.1576, wR2 = 0.3039		R1 = 0.1431, wR2 = 0.2396		R1 = 0.1410, wR2 = 0.2469	
Largest diff. peak and hole		4.487 and -2.452 e·Å^{-3}		2.015 and -1.504 e·Å^{-3}		2.257 and -1.789 e·Å^{-3}		1.796 and -1.618 e·Å^{-3}		1.965 and -1.796 e·Å^{-3}		2.179 and -1.930 e·Å^{-3}	

Table S2. Crystallographic Data and Structure Refinement parameters for compounds $LnMo_{10}$, where Ln^{III} = Tb, Dy, Ho, Er and Yb.

Compound		**$TbMo_{10}$**		**$DyMo_{10}$**		**$HoMo_{10}$**		**$ErMo_{10}$**		**$YbMo_{10}$**	
Empirical formula		$C_{69.5}H_{141.5}Cl_{4.5}Mo_{10}N_9O_{38}Tb$		$C_{69.5}H_{141.5}Cl_{4.5}DyMo_{10}N_9O_{38}$		$C_{69}H_{141}Cl_3HoMo_{10}N_9O_{38}$		$C_{72}H_{148}ErMo_{10}N_9O_{39}$		$C_{69}H_{141}Cl_3Mo_{10}N_9O_{38}Yb$	
Formula weight		2989.25		2992.83		2935.58		2890.65		2943.69	
T/K		200(1)		200(1)		200(1)		200(1)		200(1)	
Crystal system		triclinic		triclinic		monoclinic		monoclinic		monoclinic	
Space group		P -1		P -1		P 2_1/c		P 2_1/c		P 2_1/c	
a/Å	α/°	17.4477(3)	100.016(1)	17.4104(6)	100.034(2)	25.8182(6)	90	25.7069(5)	90	25.7981(4)	90
b/Å	β/°	17.8961(4)	98.861(1)	17.9043(7)	98.873(2)	21.3845(5)	106.866(1)	21.3819(4)	107.230(1)	21.3853(3)	107.070(1)
c/Å	γ/°	20.6994(4)	116.841(1)	20.6847(8)	116.854(2)	19.7951(4)	90	19.9702(3)	90	19.7968(3)	90
V/Å^3		5476.52(19)		5461.8(4)		10459.0(4)		10484.3(3)		10440.7(3)	
Z		2		2		4		4		4	
ρ_{calcd}/g cm^{-3}		1.813		1.820		1.864		1.831		1.873	
μ/mm^{-1}		1.926		1.968		2.059		2.025		2.200	
F(000)		2974		2976		5840		5772		5852	
Crystal size / mm^3		0.8 x 0.4 x 0.05		0.33 x 0.16 x 0.02		0.6 x 0.3 x 0.02		0.5 x 0.5 x 0.07		0.3 x 0.3 x 0.05	
θ range for data collection		1.036° to 30.596°		1.037° to 33.276°		0.824° to 30.608°		0.829° to 30.553°		0.826° to 33.244°	
		-24<=h<=24		-26<=h<=26		-36<=h<=36		-36<=h<=36		-39<=h<=39	
Index ranges		-25<=k<=25		-27<=k<=27		-30<=k<=30		-27<=k<=30		-32<=k<=32	
		-29<=l<=29		-31<=l<=31		-28<=l<=28		-24<=l<=28		-30<=l<=30	
Reflections collected		164098		181002		229874		181941		234650	
Independent reflections		33532 (R_{int} = 0.0267)		41999 (R_{int} = 0.0360)		32111 (R_{int} = 0.0559)		32043 (R_{int} = 0.0258)		40039 (R_{int} = 0.0310)	
Completeness		0.995		0.997		0.997		0.997		0.998	
Max. and min. transmission		0.926 and 0.525		0.932 and 0.549		0.996 and 0.625		0.916 and 0.452		0.932 and 0.549	
Data / restraints / parameters		33532 / 6 / 1237		41999 / 80 / 1215		32111 / 0 / 1226		32043 / 0 / 1200		40039 / 48 / 1233	
Goodness-of-fit on F^2		1.078		1.131		1.182		1.230		1.154	
Final R indices [I > 2σ(I)]		R1 = 0.0618, wR2 = 0.1397		R1 = 0.0487, wR2 = 0.1252		R1 = 0.0432, wR2 = 0.1014		R1 = 0.0507, wR2 = 0.0995		R1 = 0.0565, wR2 = 0.1294	
R indices (all data)		R1 = 0.0909, wR2 = 0.1763		R1 = 0.0854, wR2 = 0.1604		R1 = 0.0817, wR2 = 0.1335		R1 = 0.0789, wR2 = 0.1282		R1 = 0.0929, wR2 = 0.1719	
Largest difference peak and hole		2.727 and -2.207 e·Å^{-3}		2.820 and -1.886 e·Å^{-3}		1.727 and -1.317 e·Å^{-3}		2.186 and -1.395 e·Å^{-3}		2.258 and -2.290 e·Å^{-3}	

4. Magnetic properties

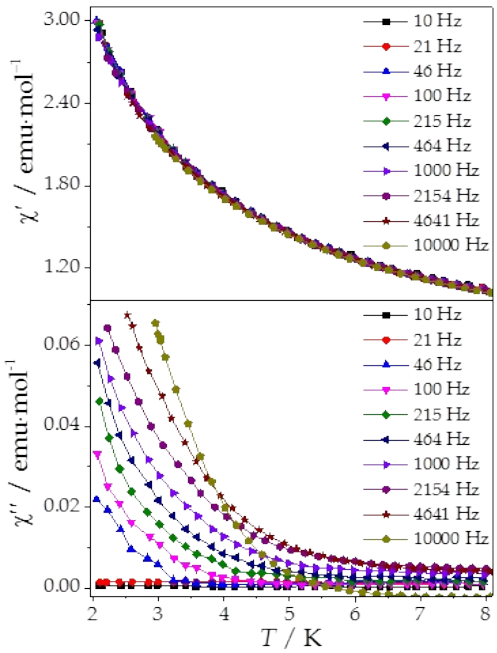

Fig. S2. In-phase (up) and out-of-phase (down) dynamic susceptibility of $HoMo_{16}$: without an external field. The frequencies are shown in the legend. Solid lines are eye-guides.

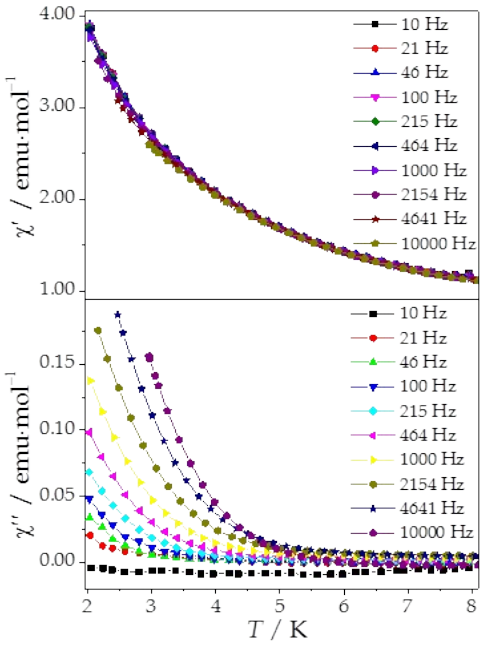

Fig. S3. In-phase (up) and out-of-phase (down) dynamic susceptibility of $ErMo_{16}$: without an external field. The frequencies are shown in the legend. Solid lines are eye-guides.

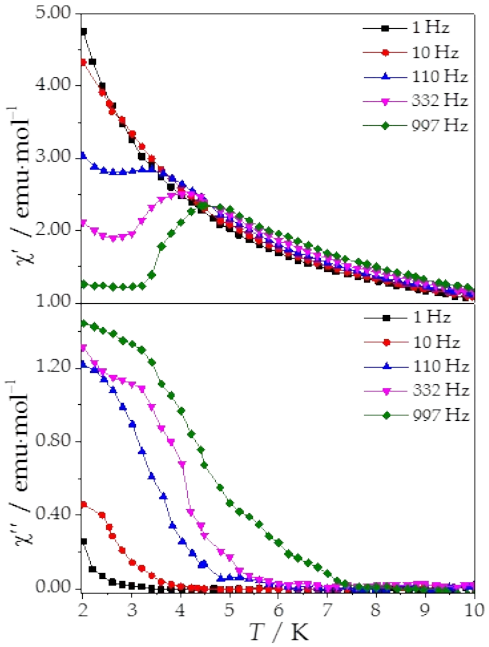

Fig. S4. In-phase (up) and out-of-phase (down) dynamic susceptibility of $DyMo_{10}$: without an external field. The frequencies are shown in the legend. Solid lines are eye-guides.

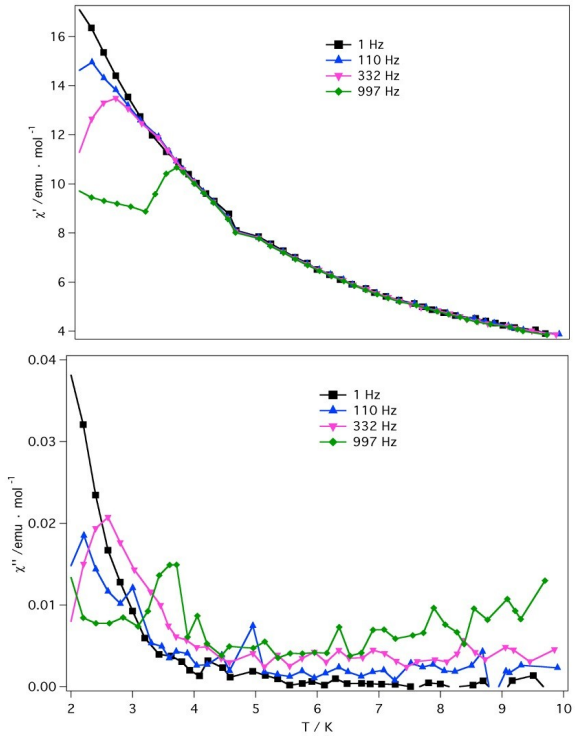

Fig. S5. In-phase (up) and out-of-phase (down) dynamic susceptibility of $ErMo_{10}$ under an external field of 1000 Oe. The frequencies are shown in the legend. Solid lines are eye-guides.

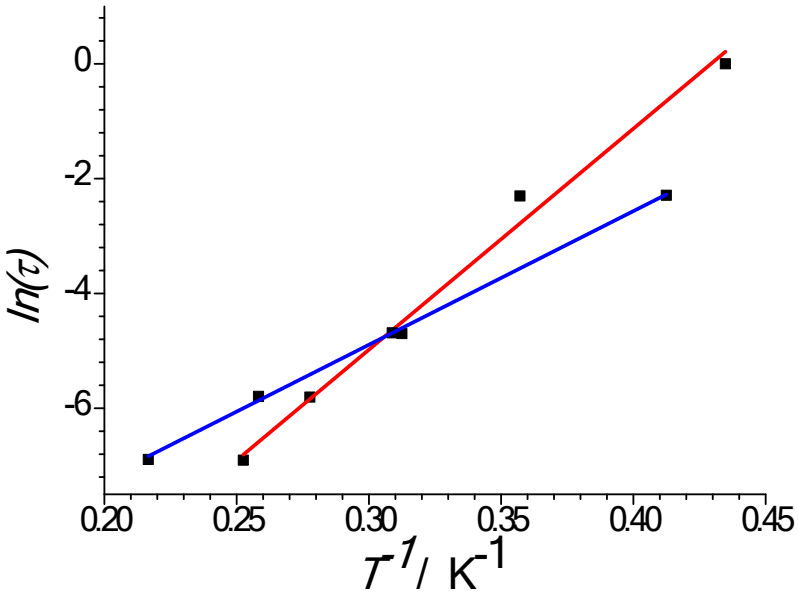

Fig. S6. Arrhenius fitting plot for $DyMo_{10}$ (red) and $YbMo_{10}$ (blue). Experimental (points) and fit (lines).

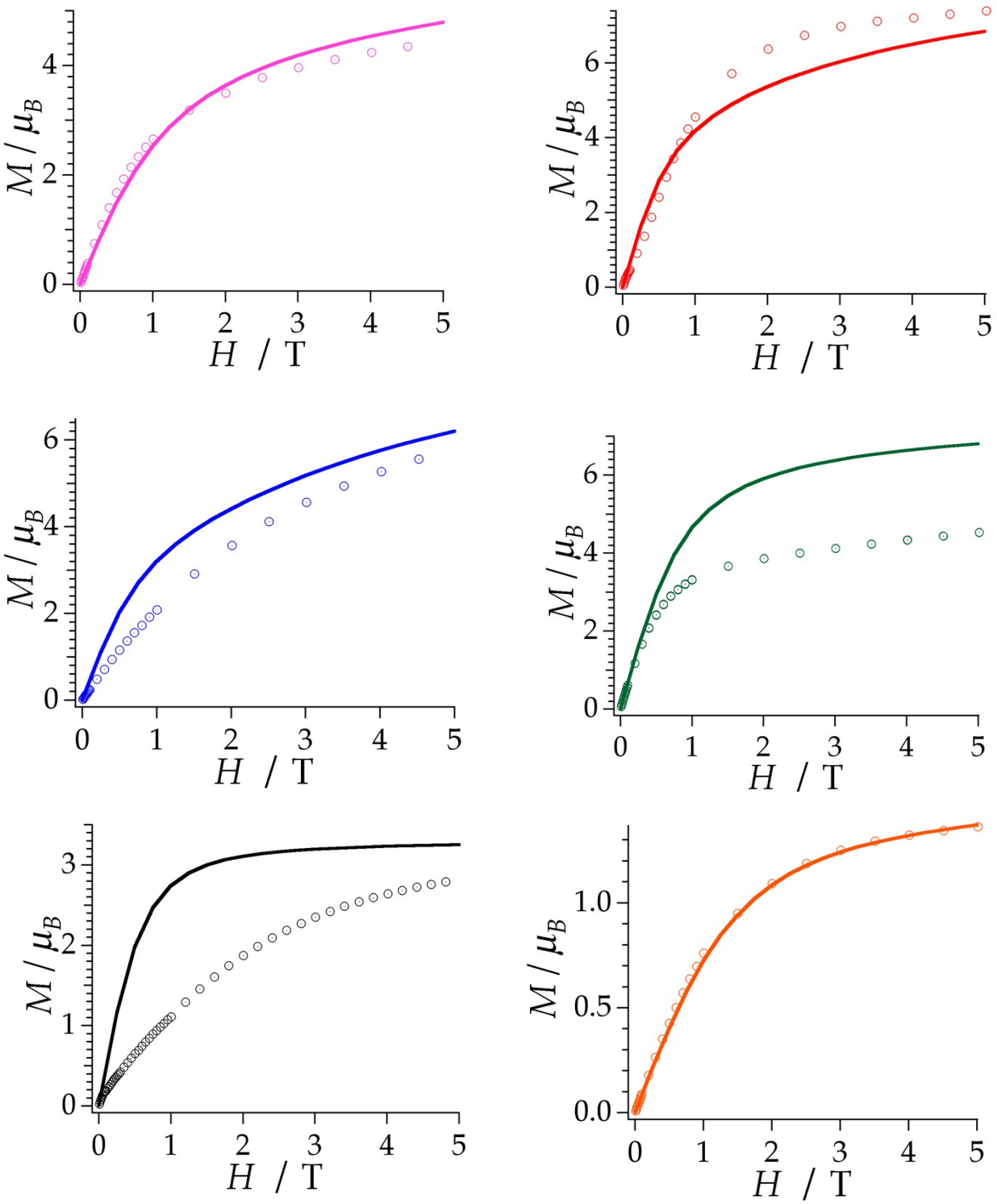

Fig. S7. Experimental (circles) and calculated (solid lines) field dependence magnetisation of $LnMo_{16}$ at 2 K measured from 0 to 5 T. Tb^{3+} (pink), Dy^{3+} (red), Ho^{3+} (blue), Er^{3+} (green), Tm^{3+} (black) and Yb^{3+} (orange).

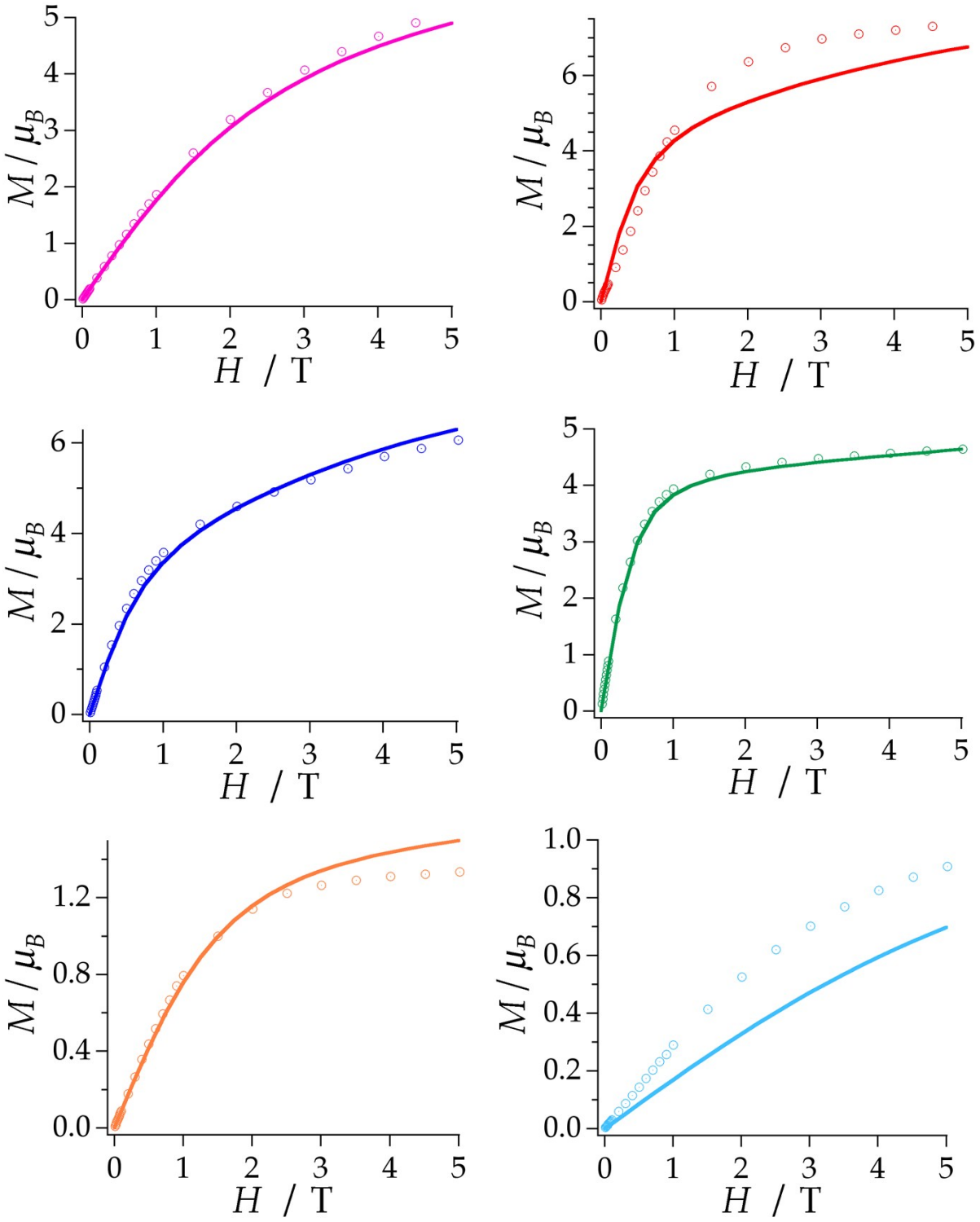

Fig. S8. Experimental (circles) and calculated (solid lines) field dependence magnetisation of $LnMo_{10}$ at 2 K measured from 0 to 5 T. Tb^{3+} (pink), Dy^{3+} (red), Ho^{3+} (blue), Er^{3+} (green), Yb^{3+} (orange) and Nd^{3+} (clear blue).

5. Mass spectroscopy

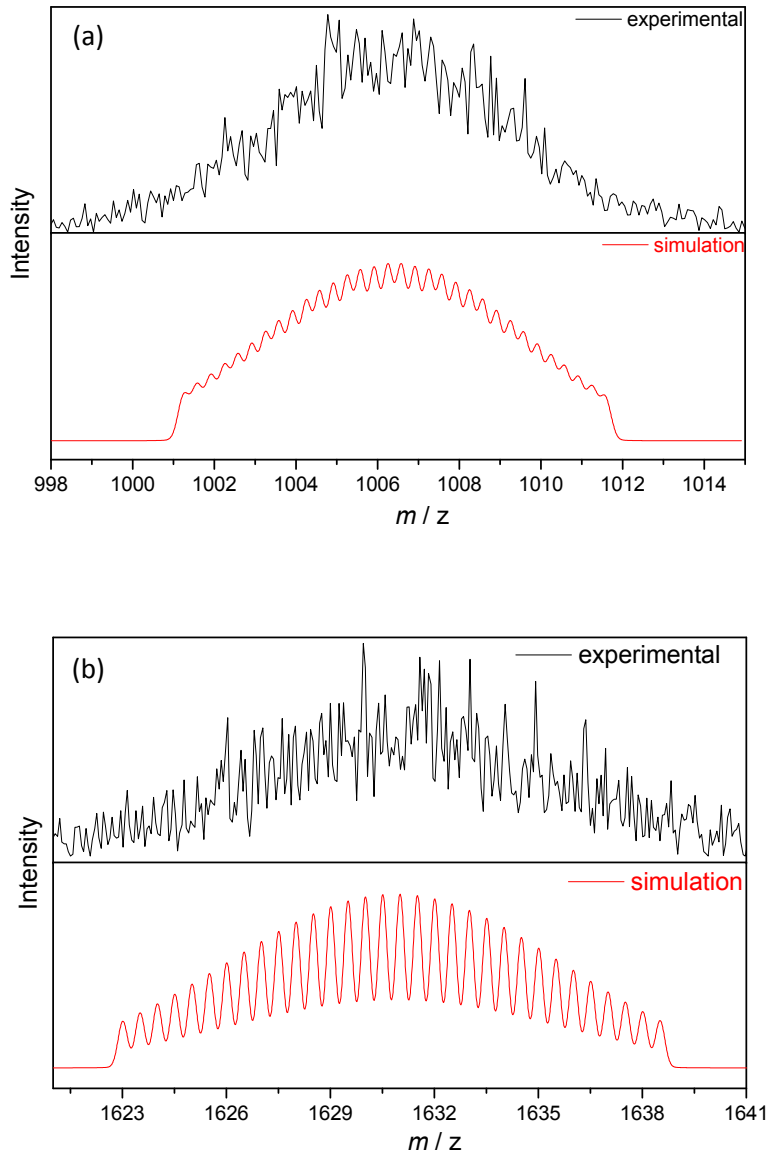

Fig. S9. Mass spectrum (ESI-MS) of $ErMo_{16}$ in negative mode in dry acetonitrile solution (up: experimental; down: simulation). (a) Expanded view of the -3 charge state, $\{TBA_2[Er(\beta\text{-}Mo_8O_{26})_2]\}^{3-}$ (*m/z* range 998-1015). (b) Expanded view of the -2 charge state, $\{TBA_3[Er(\beta\text{-}Mo_8O_{26})_2]\}^{2-}$ (*m/z* range 1160-1250).

6. Energy levels and wave functions

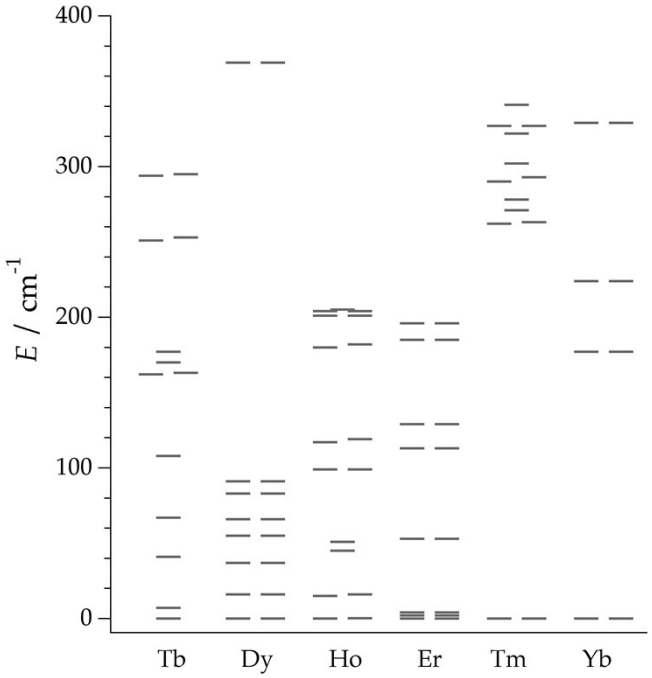

Fig. S10. Energy levels for the $LnMo_{16}$ series.

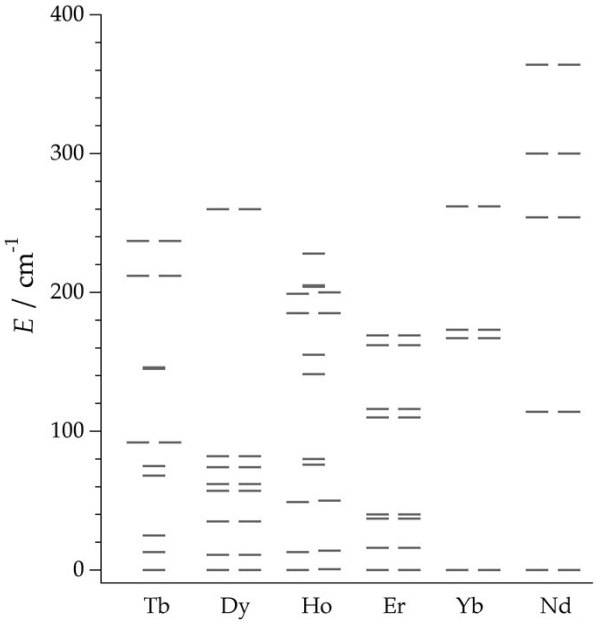

Fig. S11. Energy levels for the $LnMo_{10}$ series.

Table S3. Main contributions to the ground state wave function in the $LnMo_{16}$ series.

Tb	92% |0>
Dy	79% |±11/2> + 14% |±9/2>
Ho	47% |+4> + 47% |-4>
Er	78% |±1/2> + 12% |±13/2>
Tm	50% |+6> + 50% |-6>
Yb	99% |±5/2>

Table S4. Main contributions to the ground state wave function in the $LnMo_{10}$ series.

Tb	99% |0>
Dy	86% |±11/2>
Ho	44% |+4> + 44% |-4>
Er	99% |±15/2>
Yb	97% |±5/2>
Nd	97% |±5/2>

7. Crystal field parameters

Radial Effective Charge (REC) model

Our calculations start with the crystallographic/non-idealized atomic coordinates of the first coordination sphere of each magnetic centre. These are introduced as an input for the portable *fortran77* software code SIMPRE. This code parameterizes the electric field effect produced by the surrounding ligands, acting over the central ion, by using the following Crystal Field Hamiltonian expressed in terms of the Extended Stevens Operators (ESOs):

$$\hat{H}_{cf}(J) = \sum_{k=2,4,6} \sum_{q=-k}^{k} B_k^q O_k^q = \sum_{k=2,4,6} \sum_{q=-k}^{k} a_k (1-\sigma_k) A_k^q \left\langle r^k \right\rangle O_k^q \tag{1}$$

where k is the order (also called rank or degree) and q is the operator range, that varies between k and $-k$, of the Stevens operator equivalents O_k^q as defined by Ryabov in terms of the angular momentum operators $J_\pm$ and J_z, where the components $O_k^q(c)$ and $O_k^q(s)$ correspond to the ESOs with q ≥ 0 and q < 0 respectively. Note that all the Stevens CF parameters B_k^q are real, whereas the matrix elements of O_k^q (q < O) are imaginary. a_k are the α, β and γ Stevens coefficients for k = 2, 4, 6, respectively, which are tabulated and depend on the number of f electrons. σ_k are the Sternheimer shielding parameters of the 4f electronic shell, and $\langle r^k \rangle$ are the expectation values of the radius.

In SIMPRE, the A_k^q CF parameters are determined by the following relations

$$A_k^0 = \frac{4\pi}{2k+1} \sum_{i=1}^{N} \frac{Z_i e^2}{R_i^{k+1}} Z_{k0}(\theta_i, \varphi_i) p_{kq} \tag{2.a}$$

$$A_k^q = \frac{4\pi}{2k+1} \sum_{i=1}^{N} \frac{Z_i e^2}{R_i^{k+1}} Z_{kq}^c(\theta_i, \varphi_i) p_{kq} \tag{2.b}$$

$$A_k^q = \frac{4\pi}{2k+1} \sum_{i=1}^{N} \frac{Z_i e^2}{R_i^{k+1}} Z_{k|q|}^s(\theta_i, \varphi_i) p_{k|q|} \tag{2.c}$$

In the REC model[8] the ligand is modeled through an effective point charge situated between the lanthanoid and the coordinated atom at a distance R_i from the magnetic centre, which is smaller than the real metal-ligand distance (r_i). To account for the effect of covalent electron sharing, a radial

displacement vector ($\mathbf{D_r}$) is defined, in which the polar coordinate r of each coordinated atom is varied, $R_{eff} = r_i - D_r$. The usual procedure is to obtain the D_r parameter of each kind of donor atom from a collective fit of an observable (e.g. energy levels or magnetic properties) for a family of isostructural lanthanide complexes. At the same time, the charge value (Z_i) is scanned in order to achieve the minimum deviation between calculated and experimental data, whereas θ_i and φ_i remain constant. Due to the chemical similarity of the two families studied in this work, for the study of the series $LnMo_{10}$ we have taken advantage of the REC parametes obtained in $LnMo_{16}$. This has allowed the reduction of the number of parameters, keeping constant the product $f = D_r \cdot Z_i = 0.18216$, and varying the radial displacement to fit each lanthanoid complex of the series. The dispersion of REC parameters obtained and the function $Z_i = f / D_r$ are represented in Fig. S12.

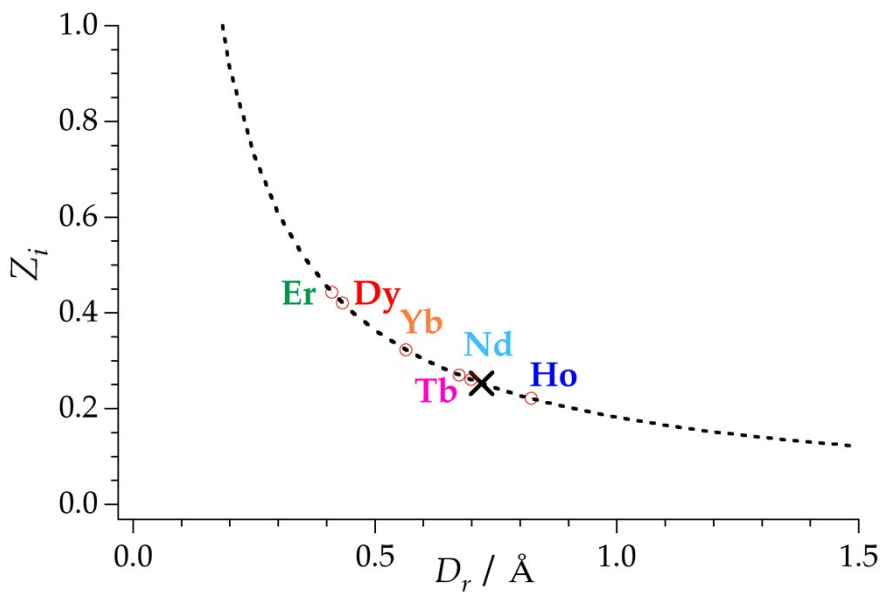

Fig. S12. Radial displacement (D_r) and effective charge (Z_i) values obtained by fitting the temperature-dependence of the magnetic susceptibility in the series $LnMo_{10}$ (circles). Collective fit of the series $LnMo_{16}$ (black cross). Function $Z_i = f / D_r$.

Table S5. Crystal field parameters obtained for the series $LnMo_{16}$.

CFP	$TbMo_{16}$	$DyMo_{16}$	$HoMo_{16}$	$ErMo_{16}$	$TmMo_{16}$	$YbMo_{16}$
$A_2^0 < r^2 >$	-170.866	-129.461	-178.319	-165.752	-185.491	-132.810
$A_2^1 < r^2 >$	127.736	-31.057	36.153	29.455	-20.933	38.885
$A_2^{-1} < r^2 >$	15.101	-29.695	-38.234	87.367	11.426	38.928
$A_2^2 < r^2 >$	-37.431	-41.117	49.594	-45.604	-39.115	41.299
$A_2^{-2} < r^2 >$	67.860	66.815	-38.973	21.692	52.151	38.889
$A_4^0 < r^4 >$	-131.564	-128.927	-121.093	-114.340	-108.688	-108.791
$A_4^1 < r^4 >$	-19.720	-118.663	-32.368	16.226	-52.638	-1.230
$A_4^{-1} < r^4 >$	32.236	92.744	-1.959	51.342	32.863	-4.515
$A_4^2 < r^4 >$	-25.121	-19.883	20.516	-21.803	-21.849	15.560
$A_4^{-2} < r^4 >$	39.566	28.215	-18.640	5.016	21.975	-17.229
$A_4^3 < r^4 >$	62.625	1.331	68.314	1.699	4.408	30.029
$A_4^{-3} < r^4 >$	167.712	-2.210	64.623	118.279	17.384	0.698
$A_4^4 < r^4 >$	-35.410	15.430	5.373	3.596	-2.255	6.833
$A_4^{-4} < r^4 >$	134.229	-26.501	-18.792	19.699	22.091	-17.191
$A_6^0 < r^6 >$	28.926	25.690	26.522	24.192	23.830	23.025
$A_6^1 < r^6 >$	-13.879	48.726	8.840	-12.026	22.444	-6.207
$A_6^{-1} < r^6 >$	-16.664	31.383	6.798	9.500	-13.844	8.106
$A_6^2 < r^6 >$	6.181	5.433	-12.563	10.401	10.194	-11.617
$A_6^{-2} < r^6 >$	-18.917	14.705	10.528	4.025	-11.782	13.070
$A_6^3 < r^6 >$	22.306	18.744	52.083	1.950	12.274	42.380
$A_6^{-3} < r^6 >$	-38.775	86.828	39.250	56.109	-49.687	15.327
$A_6^4 < r^6 >$	-22.865	14.474	-0.687	-3.954	3.964	0.171
$A_6^{-4} < r^6 >$	-73.727	16.407	-9.083	9.286	-10.342	8.011
$A_6^5 < r^6 >$	-77.229	-50.378	-125.161	-29.428	29.159	-108.165
$A_6^{-5} < r^6 >$	-54.937	216.919	73.101	135.773	-127.069	62.245
$A_6^6 < r^6 >$	1.980	-14.950	3.890	-12.112	-14.135	7.613
$A_6^{-6} < r^6 >$	-14.194	16.485	13.021	3.430	-9.251	12.099

Table S6. Crystal field parameters obtained for the series $LnMo_{10}$.

CFP	$TbMo_{10}$	$DyMo_{10}$	$HoMo_{10}$	$ErMo_{10}$	$YbMo_{10}$	$NdMo_{10}$
$A_2^0 < r^2 >$	-109.253	-107.817	-85.124	-112.554	-77.379	-167.872
$A_2^1 < r^2 >$	80.785	-23.470	44.369	-43.119	46.041	304.340
$A_2^{-1} < r^2 >$	24.181	-122.460	-40.023	-48.955	-21.661	-205.445
$A_2^2 < r^2 >$	-14.493	13.643	-0.033	5.719	-1.672	-26.369
$A_2^{-2} < r^2 >$	-13.259	-13.335	-6.000	19.016	-5.198	108.549
$A_4^0 < r^4 >$	-130.516	-97.544	-127.52	-89.564	-92.985	-274.442
$A_4^1 < r^4 >$	-24.200	-26.530	-53.751	77.562	43.125	-81.172
$A_4^{-1} < r^4 >$	-29.200	-175.595	-48.445	-24.120	18.818	90.047
$A_4^2 < r^4 >$	-7.925	19.597	-3.544	-4.402	-2.854	-19.259
$A_4^{-2} < r^4 >$	-16.633	-12.197	-7.463	9.363	-6.108	82.962
$A_4^3 < r^4 >$	-42.567	54.762	34.051	-14.763	48.178	-259.097
$A_4^{-3} < r^4 >$	53.995	6.876	30.666	-12.220	35.176	-295.856
$A_4^4 < r^4 >$	14.701	19.217	-20.406	-22.603	25.427	76.881
$A_4^{-4} < r^4 >$	23.841	-5.476	147.386	-88.748	103.827	-49.166
$A_6^0 < r^6 >$	24.573	12.995	27.339	11.910	14.051	72.191
$A_6^1 < r^6 >$	-2.625	8.973	17.232	-17.735	-16.789	-31.109
$A_6^{-1} < r^6 >$	8.086	55.949	25.174	8.605	-4.084	-2.998
$A_6^2 < r^6 >$	3.639	-10.077	0.607	0.628	0.046	12.595
$A_6^{-2} < r^6 >$	3.238	2.822	1.071	-2.440	2.832	-41.384
$A_6^3 < r^6 >$	15.802	-3.219	-68.979	15.734	-19.824	32.295
$A_6^{-3} < r^6 >$	-1.077	10.294	12.623	5.777	22.671	-13.609
$A_6^4 < r^6 >$	11.640	5.112	-23.610	-11.061	10.202	83.380
$A_6^{-4} < r^6 >$	13.561	-5.149	94.693	-34.122	45.768	-38.558
$A_6^5 < r^6 >$	-51.539	-15.974	111.850	-17.313	77.973	-302.395
$A_6^{-5} < r^6 >$	13.238	15.573	118.623	53.444	-6.327	83.759
$A_6^6 < r^6 >$	-3.096	-0.283	4.782	0.933	1.118	-7.924
$A_6^{-6} < r^6 >$	1.164	0.895	3.127	-3.310	-0.968	-26.681

8. References

1. Agilent Technologies UK Ltd, Oxford, UK, 2013, version 1.171.35.15.
2. Sheldrick, G. M. *Acta Crystallographica Section A,* **2008**, *64*, 112-122.
3. Spek, A. L. *Acta Cryst. Sect. D: Biol. Crystallogr.* **2009**, *65*, 148-155.
4. Altomare, A. ; Cascarano, G. ; Giacovazzo, C. ; Guagliardi, A. *J. Appl. Cryst.* **1993**, *26*, 343-350.
5. Farrugia, L. J. *J. Appl. Cryst.* **1999**, *32*, 837-838.